ELSEVIER

Journal of Nuclear Materials 265 (1999) 12–21

journal of nuclear materials

Vitrification of radioactive waste by reaction sintering under pressure

W.L. Gong [a], W. Lutze [a,*], A. Abdelouas [a], R.C. Ewing [b]

[a] *Center for Radioactive Waste Management (CeRaM), The University of New Mexico, 209 Farris Engineering Center, Albuquerque, NM 87131-1341, USA*

[b] *The University of Michigan, Department of Nuclear Engineering and Radiological Sciences, Ann Arbor, MI 48109-2104, USA*

Received 10 August 1998; accepted 16 October 1998

Abstract

Silicate nuclear waste glasses were synthesized by reaction sintering of powdered precursors under pressure. The glass samples contained a glass matrix phase with embedded zirconia (baddeleyite) particles. A waste composition with 38 wt% of ZrO_2 was prepared with a waste loading of 30–50 wt% at 800°C and 28 MPa, by hot isostatic pressing. The glass former was commercial amorphous silica powder to which simulated waste was added as calcined oxides. Phase compositions and microstructure of the sintered glass samples were characterized using scanning and analytical electron microscopy. The results show that extensive sintering took place and that a continuous glass phase was formed, particularly at higher waste loading. Waste components such as Na_2O, CaO, MnO_2, La_2O_3, Fe_2O_3, Cr_2O_3, and P_2O_5 dissolved completely in the glass phase. ZrO_2 was also dissolved but recrystallized from the glass as aggregates of baddeleyite crystallites surrounding the original silica particles. MCC-1 type chemical durability tests showed that the glasses are durable with dissolution rates similar to or lower than that of the highly durable French R7T7 borosilicate glass. This glass contains 13 wt% high-level radioactive waste from light water reactor fuel reprocessing and has a melting temperature of 1150°C. The long-term chemical durability of our sintered glasses is expected to be as high as that of rhyolitic glasses, based on hydration energies of 3.7 and 3.3 kJ/mole, respectively. Rhyolitic glasses show little alteration over geological periods of time with a typical corrosion rate of 1 μm/1000 yr.

1. Introduction

Currently, vitrification by melting is the only technology used to convert high-level nuclear waste (HLW) into a disposable solid [1]. The waste is mixed with glass-forming additives such as SiO_2 and B_2O_3 or a glass frit, melted and poured into steel canisters to produce a borosilicate glass. Vitrification in a ceramic melter requires that a homogeneous, single phase melt be obtained to avoid settling of solids. Crystallization can be kept to a minimum by rapid cooling to T_g, the glass transformation temperature.

There are two types of glass melters in use, metallic melters (France and England) and ceramic melters (China, Germany, Belgium, Japan, Russia, USA). Melting temperatures are limited to $\leqslant$1150°C, mainly due to rapid corrosion of critical system components such as electrodes and melter walls at higher temperatures.

The waste/glass additives ratio, i.e., the waste loading, is limited by low solubility of certain, sometimes minor waste constituents or their reaction products. There are high-level radioactive wastes that may require extensive treatment prior to vitrification by melting; otherwise, low waste loading must be accepted. Examples are certain defense wastes, e.g., some of the tank wastes at Hanford, Washington. They contain several of the following constituents at high concentrations: ZrO_2 ($\leqslant$35 wt%), Na_2O (60 wt%), Cr_2O_3 (4 wt%), Fe_2O_3 ($\leqslant$60 wt%), U_3O_8 (24 wt%) Al_2O_3 (23 wt%) Ce_2O_3 (5 wt%) and NiO (12 wt%) [2].

* Corresponding author. Tel.: +1-505 277 7964; fax: +1-505 277 9676; e-mail: brbl@unm.edu.

0022-3115/99/$ – see front matter
PII: S0022-3115(98)00654-0

Extensive research on vitrification of the Hanford tank waste by melting was conducted by Hrma and coworkers [3–7]. Their results show that Na_2O limits waste loading by lowering glass durability beyond acceptable limits. Refractory components impose prohibitive limitations on the waste loading in the glass, because of low solubility and crystallization of spinels, baddeleyite, Na–Zr–silicate, eskolaite, and possibly nepheline in the melter.

An alternative to melting is reaction sintering under pressure. The advantages of this process are: lower processing temperatures ($\leqslant 850$°C versus $\geqslant 1100$°C), little or no phase separation, less volatility of radionuclides (e.g., Cs, Mo, Te, Tc, Ru), less melter materials corrosion, and no process-related waste loading constraints. Waste loading is only limited by product quality. Potential disadvantages include the necessary use of pressure and mechanical mixing of powders under remote handling conditions.

Vitrification of high-level radioactive waste (HLW) by sintering is not new [8–12]. Sintering of HLW components into a glass matrix was first tried by Ross [13]. Terai et al. [8] investigated pressure sintering of simulated HLW with Pyrex glass frit. The chemical durability of their glass products was comparable to that of borosilicate nuclear waste glasses. At Centro Atomico Bariloche, Argentina, sintered waste glass was produced by hot uniaxial pressing in cylindrical iron cans, 140 mm in diameter [12]. Fabrication of sintered glass using hot uniaxial pressing and simulated light water reactor (LWR) and fast breeder reactor (FBR) waste, respectively, has been demonstrated in a pilot plant at the Forschungszentrum Karlsruhe (FZK), Germany, by making samples in cylindrical cans, 30 cm in diameter [9]. The highest waste loading was 35 wt%.

Recently, we reported results on vitrification by sintering under pressure with a waste loading as high as 45 wt% [14]. We are the first to use only commercially available, amorphous silica as the glass forming additive. Addition of B_2O_3 or the use of a glass frit were not required to obtain a good glass product. The chemical durability of these glasses is greater than that of melted borosilicate nuclear waste glasses. This finding is in agreement with results reported by Gahlert and Ondracek [9] who found a factor of 10 increase in chemical durability of their sintered glasses.

In this paper, we report on glasses made from powder mixtures by reaction sintering under isostatic pressure with a loading of up to 50 wt% simulated high-level radioactive waste that is typical of compositions contained in double-shell tanks (DST) at Hanford. DST-type waste contains up to 35 wt% ZrO_2. The sintered glasses were examined in terms of composition, microstructure, and chemical durability. Short-term chemical durability data are presented. Long-term chemical durability is evaluated by comparing hydration energies of our sintered glasses with those of rhyolitic glasses. Finally, the critical stages of the sintering process are discussed.

2. Experimental

2.1. Preparation of simulated DST-type waste

The estimated DST waste composition [2] and that for our simulate are given in Table 1. Zr, Ca, Mn, La, Fe, Ni, Cr, and P were introduced as crystalline oxides, Na as sodium oxalate ($Na_2C_2O_4$). Fission products and actinide elements were neglected, since their concentration is relatively small in DST waste. It can be expected that upon sintering the chemical behavior of Cs and Sr, the main radionuclides, is similar to that of Na and Ca. Actinides are represented by La. The glass former was commercial fumed amorphous silica powder (<325 mesh). Waste simulant and amorphous silica were ball-milled together using acetone as a mixing and milling medium. After 8 h of milling the product was dried in air.

Powder mixtures were characterized by measuring particle size distributions in a COULTER® LS Particle Size Analyzer. The mean particle size of the glass precursor materials varied between 0.78 and 0.81 μm. In terms of volumetric statistics, the mean size varied between 5 and 7 μm. Fig. 1 shows the particle size distribution. The powders were heated in air at 320–500°C for up to 8 h to decompose oxalate. Stirring the mixture

Table 1
Estimated average compositions in Hanford DST tank farm and simulated DST waste composition

Oxide	TF-DST	Simulated DST
SiO_2	8.31	8.90
ZrO_2	35.2	38.50
Al_2O_3	2.65	2.68
CaO	0.79	1.88
Na_2O	31.98	34.21
MnO_2	0.87	2.39
La_2O_3	0.66	0.74
Fe_2O_3	8.75	8.86
P_2O_5	0.34	0.33
F	1.43	1.51
Others [a]	9.02	0.00
Total	100.00	100.00

[a] Others include NiO 0.47, U_3O_8 2.67, B_2O_3 0.47, Cr_2O_3 0.40, and the balance 4.19 (wt%) contains ZnO, CdO, MgO, SrO, BaO, Li_2O, K_2O, Cs_2O, and Co_2O_3. In the simulated DST waste, MnO_2 represents MnO_2, NiO, Co_2O_3, and Cr_2O_3; CaO represents CaO, ZnO, CdO, MgO, SrO, and BaO; Na_2O represents Na_2O, K_2O, Li_2O, and Cs_2O; ZrO_2 represents ZrO_2 and uranium oxide. Radionuclides are not listed. Values in the second column after [2].

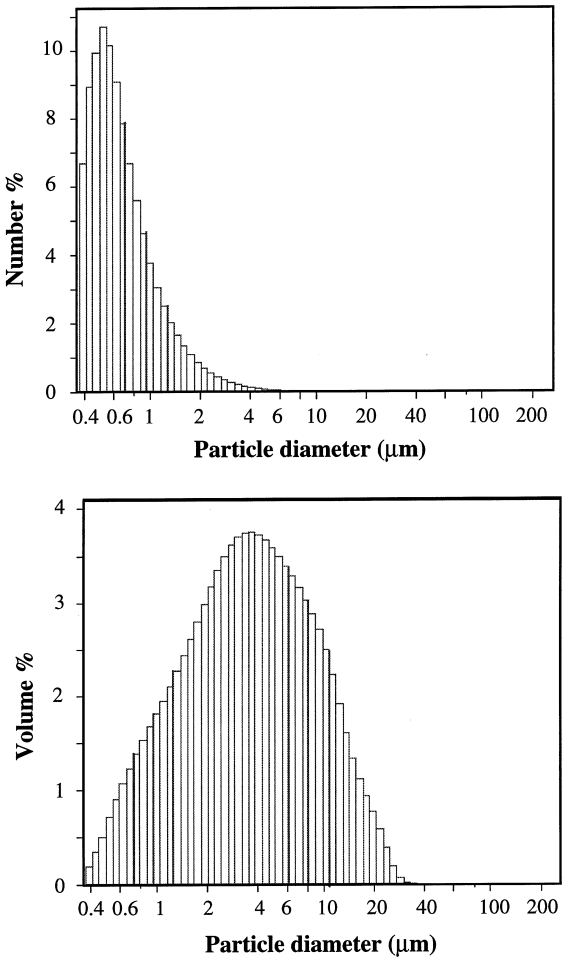

Fig. 1. Particle size of sintered glass precursors (numbers and volume density).

during heating ensured that Fe_2O_3 was not reduced. To destroy particle clusters, the heated product was ground again in a ball mill.

2.2. Cold pressing and hot isostatic pressing

Fractions of the powder mixture were compacted at room temperature in a cylindrical die (2.86 cm diameter). A pressure of 80 MPa was applied for 2 h. A cold pressed pellet weighed 12 g. It was placed into an oven inside the pressure vessel of a hot isostatic press. Argon was used as pressurizing gas. The initial setpoints of temperature and pressure were 800°C and 7 MPa. The heating rate was 27°C/min. The holding time was 1 h at 800°C. The pressure was then increased to 28 MPa. The holding time was 2 h at this pressure. The samples were cooled at a rate of 27°C/min. Five different glasses were produced with a DST waste loading up to 50 wt%, i.e. these samples were designated SG/30DST, SG/35DST, SG/40DST, SG/45DST, and SG/50DST, with the numbers representing weight of DST-type waste present.

2.3. Solid state analysis

The sintered glasses were characterized in terms of chemical composition and microstructure using scanning and transmission electron microscopy (SEM and TEM) and energy dispersive X-ray spectroscopy (EDS).

SEM work was performed on polished samples using a JMS 800 scanning electron microscope operated at 20 keV. A digitized camera was used to record secondary and backscattering electron images. The purpose of this study was to evaluate the chemical homogeneity of the glass matrix phase, to measure the composition of crystalline phases, to study the microstructure of the sintered glass samples, and to estimate porosity.

TEM work was performed with sintered glass samples using a JEM 2000FX electron microscope with a Noran TN-5500 EDS system and a JEM 2010 with an Oxford Link ISIS EDS system. The microscopes were operated at 200 keV. Most of the EDS analyses were performed using Noran's semi-quantitative analysis software package for metallurgical thin films (SQMTF). The K-factors used in the elemental corrections were calibrated in the laboratory. Final results were calculated and normalized to 100 wt%, based on the stoichiometry of oxides. Some of the EDS results were obtained using an Oxford Link ISIS EDS system attached to the JEM 2010 microscope. The analytical errors for major elements were ±5% and for others ±20%.

2.4. Chemical durability tests

The sintered glass samples were cut into a rectangular shape using an oil-lubricated low-speed diamond saw. The samples were polished with 30–1 μm diamond lapping disks. The final polishing was made using 0.05 μm colloidal silica. The glass specimens were cleaned following the MCC-1P procedure (DOE, [15]). They were washed three times in deionized water for 8 min using an ultrasonic bath, followed by two 8 min ultrasonic washes in absolute ethanol and then dried at 90°C. The geometric surface area of each specimen was measured. Then a specimen was placed in a Teflon container, deionized water was added to reach a sample surface area-to-solution volume ratio (S/V) of 10 m^{-1}. The lid was tightened. The container was weighed and placed in an oven preheated to (90 ± 1)°C. Leaching tests were run for 1, 3, 7, and 14 days. After completion of a test the container was weighed again to determine the water loss which must not exceed 10% according to the MCC-1P procedure. After cooling to room temperature the pH was measured in an aliquot of the leachate. 10 ml samples were used for chemical analysis.

To measure Na content, 1 ml of the leachate was mixed with 2 ml of 6 N HCl containing 5 g/l Cs^+ in a 10 ml volumetric flask. Water was added to reach a total volume of 10 ml. Na was measured using absorption flame spectrometry with a detection limit of 1 mg/l. Si was also measured by absorption flame spectrometry without additives to a detection limit of 1 mg/l. The normalized mass loss NL_i of element i in g/m^2, was calculated using the equation $NL_i = C_i/(f_i \cdot S/V)$ where C_i is the analyzed concentration of element i in the leachate (g/m^3) and f_i is the mass fraction of element i in the glass.

3. Results

3.1. Microstructure

The microstructure of the sintered glass consisted of a glass matrix phase with crystalline phases embedded. There was also some porosity. Fig. 2 is a SEM micrograph of a sintered glass sample with 45 wt% DST waste. Pores are visible with diameters ranging from 5 to 10 μm. The porosity was estimated to vary between 2 and 5 vol.% for all samples. Experiments have shown that the porosity can be decreased by optimizing the temperature-pressure conditions, but this was not an objective of our study. At higher magnification (Fig. 3) small white particles are visible. These consist of pure ZrO_2. Clusters of these particles are arranged in rings within the glass matrix phase. The diameter of the rings matches the size of larger silica particles (>5 μm) as they existed prior to sintering (Fig. 1). As seen in Fig. 4, the baddeleyite crystallites are about 20–40 nm in size. An electron diffraction pattern of the crystallites, shown in Fig. 4, matches that of monoclinic ZrO_2, which is baddeleyite. The size distribution of the baddeleyite particles is very narrow, more typical of precipitation from an oversaturated glass phase than of incomplete dissolution. This phenomenon will be discussed later.

The microstructures of sintered glasses with a waste loading of 30, 35, 40, and 50 wt% are similar to that shown in Figs. 3 and 4. The volume fraction of baddeleyite crystallites increases with increasing waste loading. Occasionally, undissolved Cr_2O_3 and Al_2O_3 are seen in the glass matrix.

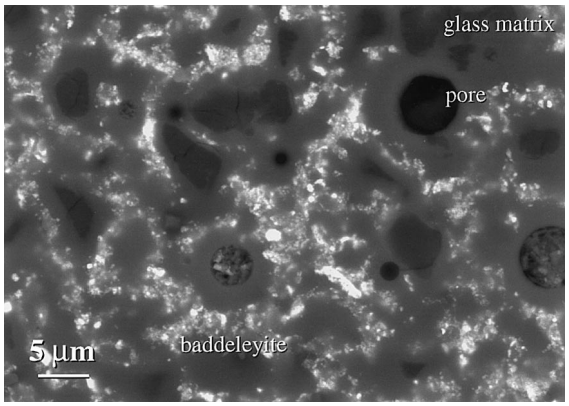

Fig. 3. SEM micrograph of sintered glass sample SG/45DST showing baddeleyite (ZrO_2) crystallites (bright) surrounding glass regions (dark).

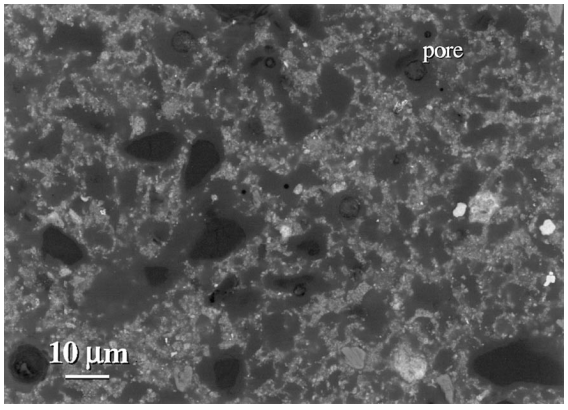

Fig. 2. SEM micrograph showing microstructure and porosity of sintered glass SG/50DST sample.

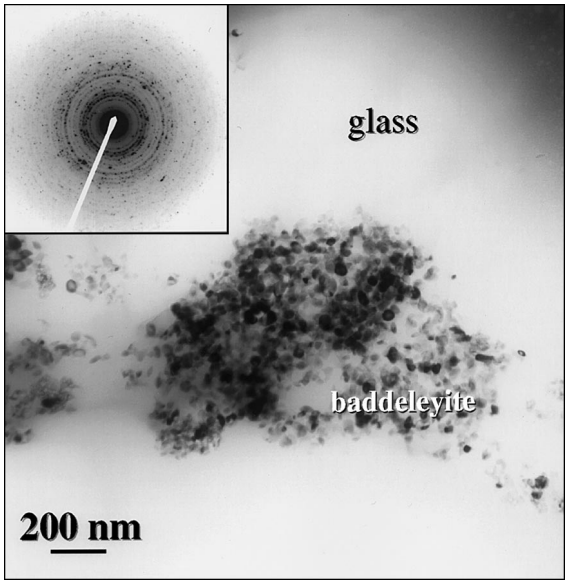

Fig. 4. TEM micrograph showing clusters of baddeleyite crystallites (~50 nm in size) in glass phase (SG/45DST). The inset is an electron diffraction pattern of baddeleyite aggregates.

3.2. Glass composition

The compositions of the glass matrix phase in our sintered samples are shown in Table 2. The main purpose of the analyses was to determine the chemical homogeneity of the glass phase. The result is that the glass is homogeneous within the limits of detection given by the EDS technique. All waste constituents became part of the glass matrix phase. Na_2O, CaO, MnO_2, La_2O_3 and Fe_2O_3 dissolved completely. Only traces of Cr_2O_3 and Al_2O_3 remained undissolved as evidenced by TEM/EDS analysis. About 60 wt% of ZrO_2 dissolved in the glass. The rest was found as pure ZrO_2 embedded in the glass phase. The solubility of ZrO_2 increased with increasing waste loading, i.e., with increasing Na content in the glass (Table 2).

Gahlert and Ondracek [9] and Andero et al. [11] reported that most of their waste elements were encapsulated as separate phases by the glass matrix phase. Embedded phases were not identified. Possible reasons for the difference with our findings include: (a) the glass forming additives are different: all authors used premelted glass frits that are less reactive then amorphous silica, e.g., sintered glass #7 (in wt%): SiO_2 72, Al_2O_3 8.6, B_2O_3 8.3, CaO 2.7, MgO 1.0, Na_2O 7.4 (Gahlert and Ondracek [9]); (b) our sintering temperature is up to 100°C higher and our pressure of 28 MPa exceeds by far the pressures used by others. Gahlert and Ondracek [8] used 1 MPa.

3.3. Chemical durability

The results of short-term chemical durability tests are given in Table 3. Fig. 5 shows the normalized mass loss of Si as a function of time for the glasses SG/35DST, SG/40DST, SG/45DST and SG/50DST. All data are for exposure at 90°C in deionized water (MCC-1P type test). The slopes of the curves correspond to the fastest dissolution rate of each glass. These results are compared with those for a French R7T7 type glass [1]. In all our tests the pH increased in the leachate (Table 3) which can be explained by Na^+/H^+ ion exchange.

The dissolution rate of the glass matrix does not depend on time in the early stages of the glass/water reaction, when the concentration of silica is low and the pH change is small. Then, the normalized mass loss of Si increases linearly with time: $NL_i = k \times t^n$ with $n = 1$. The question as to whether these conditions are met under our experimental conditions was tested by plotting $\log(NL_i)$ as a function of $\log t$. The results for SG/DST 40, SG/DST 45 and SG/DST 50 up to 7 days are shown in Fig. 6. The slope of the curve is $n = 1$, confirming a time independent dissolution rate of the glass network. The rate, $\log(NL_{Si})/\log t$, decreases with increasing waste loading between 35 and 45 wt%. At 50 wt% there was no further increase of the chemical durability. Rather, a decrease was observed. For the Na data, Fig. 7, we obtain $n = 0.8$–0.9, indicating the commonly known transition from a very short-term diffusion-controlled ion exchange ($n = 0.5$) to network dissolution ($n = 1$). Ion exchange and matrix dissolution are parallel processes. Ion exchange was indicated by an increase in pH in the leachate, up to pH = 9 after 28 days, and by the higher release of Na compared with Si (Fig. 8). From the data for Si we calculated initial glass dissolution rates ranging between 0.1 and 0.5 g/m^2/d for all sintered glasses, compared with 1.5 g/m^2/d for the R7T7 type glass [1].

4. Discussion

4.1. Chemistry and sintering mechanism

In terms of glass formation and chemical durability zirconium and sodium are the critical constituents in DST-type waste. Whereas Na enhances glass formation by supporting viscous flow, Zr has the opposite effect, regardless of initial glass composition. ZrO_2 has the strongest effect on the liquidus temperature of all oxides used in the glass industry. The melting temperature of

Table 2
The compositions of sintered glasses with 30–50 wt% of DST type waste. (All numbers in wt%)

Sintered glass	SG/30DST	SG/35DST	SG/40DST	SG/45DST	SG/50DST
Number of analyses of the glass phase	27	20	19	13	17
SiO_2	73.6	71.4	68.9	64.3	62.5
ZrO_2	8.3	8.8	8.70	10.5	10.8
Al_2O_3	0.5	0.6	0.4	0.9	1.0
CaO	0.7	0.7	0.8	1.6	1.5
Na_2O	11.2	12.9	14.4	15.0	16.9
MnO_2	0.4	0.7	0.4	1.1	1.6
La_2O_3	0.7	0.4	0.7	0.7	0.2
Fe_2O_3	4.4	4.8	5.5	6.0	5.5

Fluorine could not be measured by EDS. P_2O_5 could not be measured accurately due to its low concentration and significant peak overlap with Zr-L.

Table 3
Results of chemical durability test MCC-lP at 90°C. Normalized mass losses (NL) of Na and Si

Sintered glass	Time (d)	NL_{Na},	NL_{Si},	pH
SG/35DST	1	1.2	0.8	6.8
SG/35DST	3	1.7	0.9	7.1
SG/35DST	7	3.7	3.6	7.8
SG/35DST	14	2.4	2.9	7.3
SG/40DST	1	1.2	0.3	7.1
SG/40DST	3	3.1	1.1	7.3
SG/40DST	7	4.0	2.1	8.9
SG/40DST	14	9.5	3.2	9.0
SG/45DST	1	1.0	<0.2	7.0
SG/45DST	3	2.3	0.5	6.9
SG/45DST	7	3.5	1.0	8.9
SG/45DST	14	5.2	2.4	8.5
SG/50DST	1	3.2	0.7	8.2
SG/50DST	3	4.7	1.6	8.6
SG/50DST	7	9.5	3.5	9.1
SG/50DST	14	8.9	3.4	9.2

ZrO_2 is 2700°C, indicating a strong Zr–O bond. ZrO_2 resembles Al_2O_3 in that, like other elements with a high field strength and a directional bond, Zr strengthens the glass structure with a beneficial effect on chemical durability [16].

As sintering takes place at much lower temperatures than melting, processes such as diffusion, chemical reaction, and viscous flow are slower and homogenization of the glass matrix phase takes longer or may not be achieved at all, though supported by pressure. With increasing concentration of Na_2O, i.e., increased waste loading, the rate of glass formation and the solubility of ZrO_2 can be expected to increase.

Initially, sintering begins with Na diffusion into the amorphous SiO_2 particles, forming sodium silicate, according to the $Na_2O{\cdot}SiO_2$ phase diagram. As a result, the liquidus temperature and the viscosity of the mixed phase decrease. Viscosities of binary alkali silicate glasses are well known and can be found in text books [17]. The SiO_2–Na_2O has a eutectic at 75 mol% with a melting point of 790°C, close to our sintering temperature. The concentration of Na_2O (wt%) in this composition is 2.5 to 4 times higher than in the final glasses, depending on waste loading (Table 2). The low viscosities of the eutectic and of nearby compositions facilitate the digestion of less mobile and reactive waste

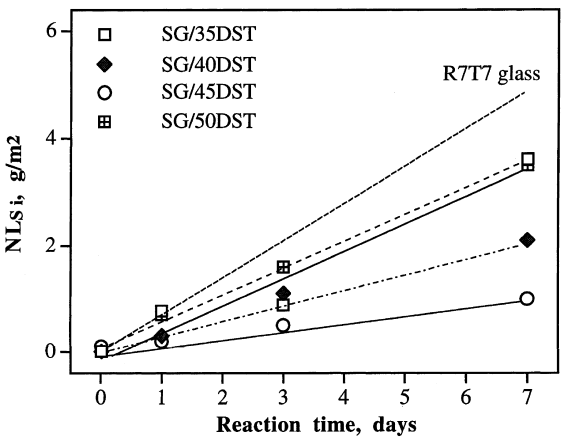

Fig. 5. Normalized mass loss of Si as a function of time (SG/35DST, SG/40DST, SG/45DST, SG/50DST, and a French R7T7 type LWR waste glass). The slope of the curves is the dissolution rate (90°C, DI water).

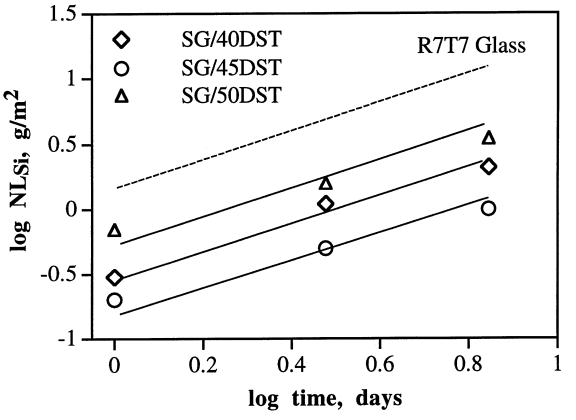

Fig. 6. Release of Si from sintered glass products SG/DST40, SG/45DST, SG/50DST and from a French R7T7 type waste glass upon leaching in deionized water over 7 days at 90°C. The slopes indicate network dissolution ($n = 1$), while the intercepts are the rates.

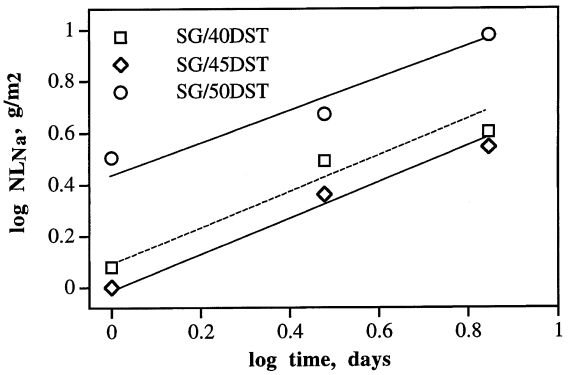

Fig. 7. Release of Na from sintered glass products SG/DST40, SG/45DST, and SG/50DST upon leaching in deionized water over 7 days at 90°C. Slopes are between 0.8 and 0.9.

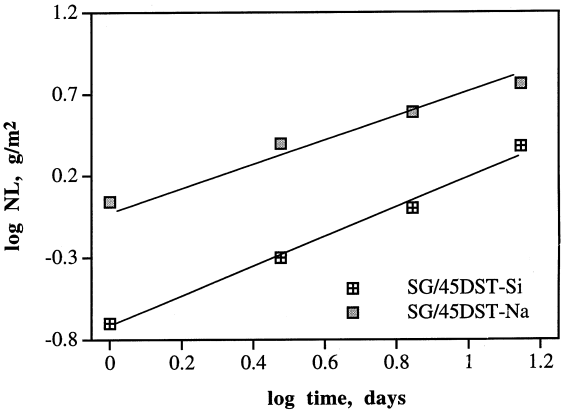

Fig. 8. Si and Na release from sintered glass product SG45/DST upon leaching in deionized water over 14 days at 90°C.

constituents than sodium. Contact of individual glass particles and formation of a glass matrix phase are enhanced by pressure. Several experiments showed that pressureless sintering results in products of higher porosity. With Na_2O concentrations >12 wt% and <35 wt% the respective melt viscosities are in the working range of glasses (10^8 dPa.s < h < 10^4 dPa.s) at 800°C. Even a commercial soda lime (window) glass meets these conditions [18]. These low viscosities explain why moderate pressures (28 MPa) are sufficient to support the sintering process effectively.

Upon digestion of other oxides the melting temperature and viscosity of the glass phase can be expected to increase. With our waste composition, the binary Na_2O–SiO_2 glass becomes essentially a ternary Na_2O–SiO_2–ZrO_2 glass with some impurities. Introducing non-bridging oxygen from Na_2O into a silica glass decreases the glass density, thereby providing space for zirconium (whose most frequent coordination number is 8), which acts as a strong network former and increases the viscosity.

As sintering continues, Na_2O is depleted in the waste and the supply to the glass phase ceases. Na^+ diffuses deeper into the silica particles and glass formation progresses. Eventually, the concentration gradient of Na between the surface and the interior of a glass particle disappears in favor of a chemically homogeneous glass. This process determines the minimal sintering time which would be 1 h for a grain size of 10 μm, if the effective Na diffusion coefficient is assumed to be on the order of 10^{-10} cm^2/s at 800°C [19]. This minimum sintering time would not allow homogenization of less mobile elements within the glass phase. The validity of this estimate was tested experimentally; after 1 h of sintering at 800°C, partially unreacted SiO_2 particles were still present in the microstructure. After 3 h reaction was complete and the glass phase was chemically homogeneous.

As the high Na/Si ratio near the glass surface decreases, this region becomes supersaturated with respect to ZrO_2 because the solubility of ZrO_2 in the glass decreases with decreasing Na_2O content in the glass. The presence of tiny baddeleyite crystals (Figs. 3 and 4) with a very narrow size distribution is taken as evidence of supersaturation followed by phase separation. Further evidence for this explanation was provided by HRTEM (Fig. 4). The formation of new crystals explains the ZrO_2 rings marking the size of the original SiO_2 particles. One would expect the ring size to be determined by the initial size of the SiO_2 particles (Fig. 1(a)). However, only particles of sufficient size and abundance are expected to dominate the microstructure of the sintered glass by providing sufficient spatial resolution for the rings to be distinguished from slightly larger ZrO_2 clusters. Empirically, we see that the effective particle sizes range between 5 and 10 μm in diameter.

We represent the DST waste glass compositions (Table 2), in an approximation, by the ternary Na_2O–ZrO_2–SiO_2 system. The three constituents represent 95.2 wt% (SG/30DST), 94.4 wt% (SG/35DST), 93.5 wt% (SG/40DST), 89.8 wt% (SG/45DST), and 89.1 wt% (SG/50DST) of the glass compositions. The actual sintered glass matrix phase has the composition Na_2O–X–ZrO_2–SiO_2 where X represents all other oxides listed in Table 1 (4.8 wt% $\leqslant$ X $\leqslant$ 10.9 wt%). X includes also the precipitated fraction of ZrO_2. In the Na_2O–ZrO_2–SiO_2 system the maximum solubility of ZrO_2 is about 20 wt% [20,21]. The solubility of ZrO_2 at the high SiO_2 and relatively low Na_2O concentrations in our DST-type waste glasses increases from 8 to 11 wt% when the Na_2O content increases from 11 to 17 wt% (Table 2). The total concentration of ZrO_2 in the sintered glass product increases from about 11 wt% (SG30/DST) to about 17 wt% (SG50/DST). Taking these numbers and subtracting the measured ZrO_2 solubilities allows us to calculate the phase composition of the sintered glass product. This

composition ranges between 97 wt% glass and 3 wt% ZrO_2 (SG30/DST) and 94 wt% glass and 6 wt% ZrO_2 (SG50/DST). The fact that ZrO_2 crystals are in contact with the glass phase and that there is no detectable concentration gradient of Zr within the glass phase, as evidenced by EDS line scans, indicates that ZrO_2 reached its maximum concentration in all glasses. Introducing the other waste elements into the Na_2O–ZrO_2–SiO_2 system may lower the solubility of ZrO_2. For example, in the ternary system Na_2O–CaO–SiO_2 the maximum solubility of ZrO_2 is 8 wt%. As the number of non-bridging oxygen produced by dissolution of Na_2O in amorphous silica is limited, other network forming elements such as Fe may compete with Zr for structural sites in the glass.

4.2. Short-term chemical durability

Addition of ZrO_2 to a glass increases its chemical durability. Zr is added to many commercial glasses in different concentrations, typically between 0.5 and 15 wt%. These glasses are melted at temperatures much higher than those applicable to nuclear waste vitrification ($\geqslant 1400$°C). Therefore, the chemical durability of nuclear waste glasses cannot be improved substantially by just adding enough ZrO_2. The alkali oxides Li_2O and Na_2O, commonly present in waste glass frits and in many wastes, deteriorate the chemical durability of a glass unless their adverse effect is mitigated by elements that improve the glass chemical durability. With an upper boundary of 1150°C for the melting temperature, the possibilities to improve chemical durability are limited. Here, vitrification of high-level radioactive waste by sintering offers a clear advantage over melting. As an example, Table 3 shows that the chemical durability increases instead of decreasing with increasing Na concentration in the glass. The increasing concentration of ZrO_2 overcompensates the deleterious effect of Na_2O. At 45 wt% waste loading, the initial glass dissolution rate, k, is a factor of 15 lower than that of the R7T7 type glass (Fig. 6). The release rate, k, measures an intrinsic glass property and depends only on glass composition, if temperature and pH are constant. The increase in the pH as the glass/water reaction progresses is relatively small in the first days but is different for the different glasses. This was neglected when comparing the k values.

4.3. Long-term chemical durability

Our short-term leaching tests do not provide information on the long-term chemical durability of the sintered glasses. Therefore, we have searched for a suitable natural analogue for these silicate glasses. Based on chemical composition, rhyolitic glasses (obsidians) have been selected. Rhyolitic glasses do not contain appreciable amounts of Zr but they do contain Al. Both Al and Zr enhance the chemical durability of a glass, Zr more so than Al. Except for ZrO_2, rhyolitic glasses have comparable compositions to our waste glasses.

The chemical composition of rhyolitic glasses from different locations is given in Table 4. The table shows that the compositions of rhyolitic glasses do not vary greatly between locations. The sum of the major elements SiO_2 and Al_2O_3 in weight percent ranges between 85% and 89%. The sum of the alkaline oxides Na_2O and K_2O varies between 7% and 10%. Contents of Fe_2O_3 and CaO are less than 3% and 2%, respectively. Freshly erupted glasses contain some water, typically less than 1%.

Rhyolitic glasses occur in nature as a result of rapid cooling (quenching) of silicate melts (magmas) as they come into contact with a quenching medium (water, ice, atmosphere). Rhyolitic glasses have been studied to extract information relevant to the evaluation of the long-term chemical durability of nuclear waste glasses

Table 4
Chemical composition of rhyolitic glasses from different locations (in wt%)

Element	Glass 1	Glass 2	Glass 3	Glass 4	Glass 5	Glass 6	Glass 7	Glass 8	Glass 9	Glass 10
SiO_2	76.7	73.1	76.0	73.1	75.4	74.67	73.03	72.11	75.32	74.4
Al_2O_3	12.5	11.9	13.5	11.9	12.9	12.17	12.37	14.16	11.92	12.7
Fe_2O_3	0.43	2.4	1.6	2.6 *	1.0	3.21	2.67	3.17	3.42	1.60
Na_2O	3.3	3.5	4.5	3.5	4.1	4.25	5.29	5.47	4.14	3.77
K_2O	4.6	4.5	3.5	4.5	4.4	2.78	4.84	4.33	2.60	4.75
CaO	0.48	2.6	0.7	2.6	0.6	1.68	1.31	0.69	1.66	0.70
MgO	0.09	1.0	0.3	1.0	0.1	0.10	0.15	0.03	-	0.04
TiO_2	-	0.2	0.28	0.2	0.1	0.30	0.23	0.19	-	0.60
H_2O	0.30	-	-	-	-	-	-	0.15	-	-

Glass 1: Friedman and Long [35], Yellowstone, Montana – Glass 2: Ewing [36], no location given – Glass 3: Malow et al. [37], Glass Mountain, Siskiyou County, California – Glass 4: Lutze [1], no location given, *MnO + Fe_2O_3 – Glass 5: Thomassin and Iiyama [38], Wada-Toge, Japan – Glass 6: Petit et al. [39], no location given – Glass 7: Stevenson and McCurry [40], New Mexico – Glass 8: Mazer et al. [41], Orito Quarry, Easter Island – Glass 9: Magonthier et al. [25], Myvatn area, northern Iceland – Glass 10: Abdelouas [26], Lipari, Italy.

[22–26]. The alteration of rhyolitic glasses is the first step of the formation of many volcanic and sedimentary ores [27–29]. Magonthier et al. [25] studied the natural corrosion of 52 000 year old Icelandic obsidian and reported that: (1) the corrosion rate of obsidian at 10°C and below is about 1.1 μm/1000 yr, in good agreement with data published in the literature (e.g. Friedman and Trembour [30]); (2) the long-term corrosion rate is controlled by ion diffusion. Abdelouas [26] studied rhyolitic glasses naturally corroded in salt lakes in Bolivia and showed that the secondary phases (Sr-rich barite, cerianite, Mg-rich smectite) in the obsidians are similar in structure and composition to those seen in the French reference nuclear waste glass R7T7 corroded in saline solutions in the laboratory. The glass corrosion rate of a 30 000 year old sample was estimated to be (0.045 ± 0.015) μm/1000 yr at 10°C.

In Table 5 we show average compositions of sintered glasses and the average compositions of rhyolitic glasses from Table 4. This table shows that both glasses are mainly composed of three oxides. In rhyolitic glasses these are SiO_2, Al_2O_3 and R_2O (R = Na, K); in our waste glasses the dominant oxides are SiO_2, ZrO_2 and Na_2O. These oxides constitute 93–95 wt% of the glass compositions. As a first approximation, properties of the rhyolitic glasses can be discussed on the basis of the ternary Na_2O–Al_2O_3–SiO_2 system, while those of the waste glasses are related to the Na_2O–ZrO_2–SiO_2 system. The average molar composition of the waste glasses is 0.2 Na_2O, 0.08 ZrO_2, 1.25 SiO_2, while that of rhyolitic glasses is 0.06 Na_2O (0.1 R_2O), 0.12 Al_2O_3, 1.25 SiO_2. On a molar basis, in rhyolitic glasses, the ratio of Al_2O_3 : Na_2O = 2:1, or close to 1, if R_2O is considered R = Na, K). Al is expected to be present in tetrahedral (network former) and octahedral coordination (network modifier) as the above ratio is >1.

The main differences in the chemical compositions are reflected in the presence of Zr and a relatively high content of alkali (Na) in the waste glass versus a much higher Al and a lower alkali (Na + K) content in the natural glass (Table 5). To quantify these differences we calculated the free energy of hydration for both glasses, using Paul's [31] method. Thermodynamic data for these calculations were published by Jantzen and Plodinec [32]. The results at 25°C are given in Table 5, where it can be seen that the ΔG°_{hyd} values are almost the same.

Table 5
Average compositions of rhyolitic and sintered glasses and free energies of hydration

Elements	Sintered glasses	Rhyolitic glass
SiO_2	68.1 ± 3.8	74.4 ± 1.2
Al_2O_3	0.7 ± 0.2	12.6 ± 0.6
Fe_2O_3	5.2 ± 0.5	2.2 ± 0.8
Na_2O	14.1 ± 1.6	4.2 ± 0.6
CaO	1.1 ± 0.4	1.3 ± 0.7
ZrO_2	9.4 ± 1.0	-
MnO_2	0.8 ± 0.4	-
La_2O_3	0.5 ± 0.2	-
K_2O	-	4.0 ± 0.7
MgO	-	0.3 ± 0.3
ΔG°_{hyd} (kJ/mole)	3.7	3.3

The contribution of silica in the hydration energy of the glass is similar for rhyolitic glasses (ΔG°_{hyd}(silica) = 16.8 kJ/mol) and nuclear waste glasses (ΔG°_{hyd}(silica) = 12.6–14.6 kJ/mol). Aluminum improves the chemical durability of silicate glasses [33,34]. Only at high concentrations is there a deleterious effect from the network modifying fraction of Al. Zr increases the durability of silicate glasses more than any other element commonly used in the glass industry. Assuming that ZrO_2 forms a structural environment in the glass similar to that in $ZrSiO_4$ (ΔG°_{hyd}(Zr) = 8.5–9.1 kJ/mol), the stronger stabilizing effect of Zr compared with Al_2O_3 in the glass becomes evident (ΔG°_{hyd}(Al) = −2.6 kJ/mol). Increasing the Na content of nuclear waste glasses (ΔG°_{hyd}(Na_2SiO_3) = −18.79–−14.4 kJ/mol) leads to a decrease in the hydration energy (lower chemical durability). The sum of the alkalis (R_2O) in the rhyolites yields a ΔG°_{hyd}(Na + K) = −10.5 kJ/mol. Small amounts of Fe_2O_3 have little effect on the durability, as described by Feng et al. [34]. The contribution of Fe_2O_3 to the hydration energy is similar for both rhyolitic and nuclear waste glasses. The effect of CaO, MgO, and other oxides (Table 1) is negligible because of their low concentrations. Based on these calculations, we assume that the long-term durability of our waste glasses can be evaluated based on corrosion features seen in rhyolitic glasses.

5. Conclusions

Vitrification by reaction sintering under pressure is a promising alternative to melting, if the radioactive waste contains a large amount of refractory oxides such a ZrO_2 and Cr_2O_3. Sintered glasses with a waste loading as high as 50 wt% were obtained at a processing temperature of 800°C and a pressure of 28 MPa. All waste constituents except Zr were homogeneously dissolved in the glass phase. About 60% of the initial ZrO_2 dissolved in the glass matrix; the rest precipitated by a complex mechanism as baddeleyite crystallites formed along the original grain boundaries of silica particles. Baddeleyite crystallites form by supersaturation in an early stage of the sintering process. The sintered glasses can be represented by a ternary Na_2O–ZrO_2–SiO_2 system. The high silica (63–74 wt%) and zirconia (8–11 wt%) contents of the glasses explain their high chemical durability. The deleterious effect of Na on chemical durability is more than compensated by the beneficial effect of Zr. Long-term chemical durability of the sintered glasses is expected to be high, based on the similarity of hydration

energies of rhyolitic and the sintered glasses. The corrosion rate of rhyolitic glasses in various natural environments has been shown to be very low, namely 1 μm/1000 yr.

Although hot pressing of sufficiently large volumes can be accomplished with state of the art technology, remote handling in a radioactive environment remains to be demonstrated.

References

[1] W. Lutze, in: W. Lutze, R.C. Ewing (Eds.), Radioactive Waste Form for the Future, North-Holland, New York, 1988, p. 1.
[2] The Hanford Site Tank Waste Remediation System: an Update, Westinghouse Hanford, Report # WHC-SA-2124, 1996.
[3] P. Hrma, R.J. Robertus, Ceram. Eng. Sci. Proc. 14 (1993) 187.
[4] P. Hrma, Ceram. Trans. 45 (1994) 391.
[5] P. Hrma, G.F. Piepel, P.E. Redgate, D.E. Smith, M.J. Schweiger, Ceram. Trans. 61 (1995) 505.
[6] P. Hrma, J.D. Vienna, M.J. Schweiger, Ceram. Trans. 72 (1996) 449.
[7] Q. Rao, G.F. Piepel, P. Hrma, J.V. Crum, J. Non-Cryst. Solids 220 (1997) 17.
[8] R. Terai, M. Kinoshita, K. Eguchi, Osaka Kogyo Gijutsu Shikenjo Kiho 29 (1978) 36.
[9] S. Gahlert, G. Ondracek, in: W. Lutze, R.C. Ewing (Eds.), Sintered Glass in Radioactive Waste Form for the Future, North-Holland, New York, 1988, pp. 162–192.
[10] M. Nishioka, S. Hirai, K. Yanagisawa, N. Yamasaki, J. Am. Ceram. Soc. 73 (1990) 317.
[11] M.A. Andero, A.M. Bevilacqua, N.B.M. de Bernasconi, J. Nucl. Mater. 223 (1995) 151.
[12] A.M. Bevilacqua, N.B.M. de Bernasconi, D.O. Russo, M.A. Audero, M.E. Sterba, A.D. Heredia, J. Nucl. Mater. 229 (1996) 187.
[13] W.A. Ross, Report No. BNWL-SA-5362, Battelle Pacific Northwest Laboratories, Richland, 1975.
[14] W. Lutze, W.L. Gong, A. Abdelouas, R.C. Ewing, C. Scales, Mater. Res. Soc. Symp. Proc., 506 (1998) 223.
[15] DOE, MCC-1 Static Leach Test Method, Nuclear Waste Materials Handbook, DOE/TIC-11400, 1982.
[16] M.B. Volf, Chemical approach to glass, in: Glass Science and Technology, vol. 7, Elsevier, New York, 1984.
[17] W. Vogel, Glas Chemie, 3rd ed., Springer, Berlin, 1992.
[18] R.H. Doremus, Glass Science, 2nd ed., Wiley, New York, 1992.
[19] O.V. Mazurin, M.V. Streltsina, T.P. Shvaiko-Shvaikovskaya, Handbook of Glass Data, Part A: Silica Glass and Binary Silicate Glasses, Elsevier, New York, 1983.
[20] G. D'ans, G. Löffler, Z. Anorg. Allgem. Chem. 191 (1930) 22.
[21] W. Eitel, M. Pirani, K. Scheel, Glastechnische Tabellen, Springer, Berlin, 1932.
[22] R.A. Zielinski, Nucl. Tech. 51 (1980) 197.
[23] A.P. Dickin, Nature 294 (1981) 342.
[24] R.C. Ewing, J.C. Jercinovic, Mater. Res. Soc. Symp. Proc. 84 (1987) 67.
[25] M.-C. Magonthier, J.C. Petit, J.-C. Dran, Appl. Geochem., Suppl. Issue No. 1 (1992) 83.
[26] A. Abdelouas, PhD thesis, The University of Strasbourg, France, 1996.
[27] D.M. Burt, M.F. Sheridan, Am. Assoc. Petrol. Geol. Studies Geol. 13 (1981) 99.
[28] R.A. Zielinski, in: Uranium Deposits in Volcanic Rocks, IAEA, vol. 83, 1985, Vienna.
[29] M.-C. Magonthier, Bull. Soc. Fr. Miner. Cristallogr. 110 (1987) 305.
[30] I. Friedman, F.W. Trembour, Am. Sci. 66 (1978) 44.
[31] A. Paul, J. Mater. Sci. 12 (1977) 2246.
[32] C.M. Jantzen, J.M. Plodinec, J. Non-Cryst. Solids 67 (1984) 207.
[33] A. Paul, M.S. Zaman, J. Mater. Sci. 13 (1978) 1399.
[34] X. Feng, I.L. Pegg, A. Barkatt, P.B. Macedo, S.J. Cucinell, S. Lai, Nucl. Tech. 85 (1989) 334.
[35] I. Friedman, W. Long, Science 191 (1976) 347.
[36] R.C. Ewing, Mater. Res. Soc. Symp. Proc. 1 (1978) 57.
[37] G. Malow, W. Lutze, R.C. Ewing, J. Non-Cryst. Solids 67 (1984) 305.
[38] J.H. Thomassin, T. Iiyama, Bull. Minéral. 111 (1988) 633.
[39] J.C. Petit, G. Della Mea, J.C. Dran, M.C. Magonthier, P.A. Mando, A. Paccagnella, Geochim. Cosmochim. Acta 54 (1990) 1941.
[40] C.M. Stevenson, M.O. McCurry, Geoarcaeol. 5 (2) (1990) 149.
[41] J.J. Mazer, C.M. Stevenson, W.L. Ebert, J.K. Bates, Am. Antiq. 56 (3) (1991) 504.